Multi-objective optimization design of wheat centralized seed feeding device based on particle swarm optimization (PSO) algorithm

Qingqing Wang[1], Zhaodong Li[1,2], Weiwei Wang[1,2], Chunling Zhang[1,2],
Liqing Chen[1,2*], Ling Wan[1,2]

(1. *College of Engineering, Anhui Agricultural University, Hefei 230036, China*;
2. *Anhui Province Engineering Laboratory of Intelligent Agricultural Machinery and Equipment, Hefei 230036, China*)

Abstract: In order to solve the problem of interaction between multiple evaluation indexes of seed metering performance under multiple factors of centralized seed feeding device, a multi-objective optimization of structure based on particle swarm optimization (PSO) algorithm was proposed in this paper. The wheat centralized seed feeding device was taken as the research object, and the experimental factors were cone angle of type hole, working speed and seed filling gap. The working process of wheat centralized seed feeding device was simulated by discrete element method (DEM). The average seed number of type hole, the variation coefficient of the average seed number of type hole, and the maximum tangential force between seed and seed feeding mechanism were selected as the evaluation indexes. Through the variance analysis of the evaluation indexes by the experimental factors, the optimization objective function was constructed. Using PSO algorithm, the multi-objective optimization was carried out for the wheat centralized seed feeding device. The optimization results show that the best structural combination parameters of the wheat centralized seed feeding device are the hole cone angle of 31.6° and the seed filling gap of 4.6 mm. The validity of the method was verified by simulation and field test. The results show that the PSO algorithm multi-objective optimization method proposed in this paper can provide a reference for the structural improvement and optimal design of the centralized seed feeding device.
Keywords: centralized seed feeding device, multi-objective, optimization, PSO algorithm
DOI: 10.25165/j.ijabe.20201306.5665

1   Introduction

Wheat high-speed quantitative sowing technology has the advantages of saving time, saving cost and high efficiency, which has become the development direction of wheat machinery planting in Huang-Huai Region of China. As the core part of the pneumatic seeder, the wheat centralized seed feeding device has the advantages of strong seed adaptability, low seed injury rate and easy to achieve precision and wide in width operation, which has become the mainstream of the future development of the seeder. Scholars at home and abroad have carried out fruitful research on this[1-4]. Anantachara et al.[5] and Karayel et al.[6] optimized the structure of the seed chamber to improve the seed filling performance. Lei et al.[7,8] used DEM-CFD coupling method to analyze the influences of Venturi throat area, throat length, air inlet

velocity and seed rate on the operation efficiency of pneumatic collective row seeder from two aspects of air field and seed movement. In order to reduce the complexity of the set row seeder, Liao et al.[9] developed a new type of precision seed metering device with inner inflation. Zhang et al.[10] designed a kind of seed suction plate with hole group by using the combination of positive and negative air pressure to improve the precision of seed metering. Andrii et al.[4] studied the effects of air velocity, material flow rate, angle position of distributor head and different outlet pipe length on the distribution accuracy of distributor head. Han et al.[11] used the method of DEM-CFD coupling to analyze the primary and secondary factors of the location, width and average arc length of the lateral hole that affect the performance of the inner filling corn metering device. Liu et al.[12] designed a pinhole wheat precision sowing device and its seed absorption performance was studied. In the field of different disciplines, multi-objective optimization is more and more widely used. Zhou et al.[13] using the approximate model and genetic algorithm, the multi-objective optimization of the structure of tilt table maneuver of multirotor unmanned aerial vehicle (MUAV) is carried out to improve its lightweight and control accuracy. Hrvoje et al.[14] used the multi-objective optimization method to analyze the influence of fire and tax on the natural gas consumption of adiabatic boiler. Paul et al.[15] proposed a multi-objective optimization method aiming at the optimization problem in the design process of nuclear power plant. For the problem of gear ratio and torque distribution in the electric vehicle with two motors, the multi-objective optimization was carried out by Kihan et al.[16]

with the acceleration time and energy consumption as the evaluation indexes. The above shows that experts at home and abroad have made rich achievements in the study of pneumatic seed metering, but most of the existing studies are limited to the optimization of an evaluation index by a certain factor or several factors. In the actual working process of seeder, many evaluation indexes interact with each other, such as seed filling performance of seed metering device, coefficient of variation of seed metering and seed breakage rate. Therefore, further discussion is needed in this respect. In the calculation of multi-objective optimization, it is easy to fall into the local optimal value, so a global solution is needed. Particle swarm optimization (PSO) is one of the most popular optimization categories at present. Its principle is to find the global optimal solution by imitating the natural biological foraging process, which is used to provide innovative solutions to complex problems[17-19].

In brief, many experts have achieved some results in the aspect of centralized seed feeding device, but the multi-objective optimization influenced by interaction factors needs further discussion. Therefore, based on the concept of multi-objective optimization, this paper takes the previously designed wheat centralized seed feeding device as the research object[20], mainly doing the following work: (1) put forward the key experimental factors of seed filling gap, and discussed the influence law of seed filling gap, cone angle of type hole and working speed on the tender delivery of the central seeder, (2) constructed the multi-objective optimization function including average seed number of type hole, variation coefficient of the average seed number of type hole and maximum tangential force between seed and seed feeding mechanism; (3) based on the PSO algorithm considering the weight coefficient, the objective function is optimized. According to the optimization results, the field test was carried out. Therefore, this study can provide a reference for the structure design and performance improvement of the centralized metering device.

2 Working principle of wheat centralized seed feeding device

The structure of air-assisted centralized seed feeding system was composed of high pressure blower, seed box, centralized seed feeding device, Venturi feeding device, seed conveying pipe, booster pipe, distribution head, etc. as shown in Figure 1a. At working status, the high-pressure blower is used as the air supply device to continuously provide the required air pressure; the seeds of seed box were transported quantitatively by wheat centralized seed feeding device and fall into Venturi tube; under the action of air pressure, the seeds are dispersed and decelerated by the booster pipe and then move to the distributor; distributor to disperse the seeds with equal feasibility; the seeds of wheat were sown into the soil through the seed delivery pipe and the double disc ditcher, shown in Figure 1b.

The core working part of the air-assisted centralized seed feeding system is a centralized seed feeding device, which is mainly composed of seed box, seed feeding shell, seed filling chamber, seed filling regulating plate and seed feeding mechanism, as shown in Figure 2a. The seed feeding mechanism mainly includes type hole wheel, blank wheel, diaphragm and transmission shaft, as shown in Figure 2b. When sowing, the wheat seeds in the seed box enter the seed filling chamber under the action of gravity, and the seeds in the seed filling chamber are filled into the holes of the type hole wheel of the seed feeding mechanism under the action of the lateral pressure of the seed population and the type

hole disturbance, and rotate with the type hole. The seeds in the type hole and the seeds carried by the seed flow complete the precise filling through the seed filling gap formed by the seed filling adjusting board and the seed feeding mechanism. With the rotation of the type hole wheel, wheat seeds fall into the Venturi tube through the seed fall mouth under the action of gravity and centrifugal force to complete the supply of wheat seeds.

1. High pressure blower   2. Seed box   3. Wheat centralized seed feeding device   4. Venturi tube   5. Booster pipe   6. Distributor   7. Seed delivery pipe   8. Double disc ditcher
a. Composition structure

b. Working principle block diagram
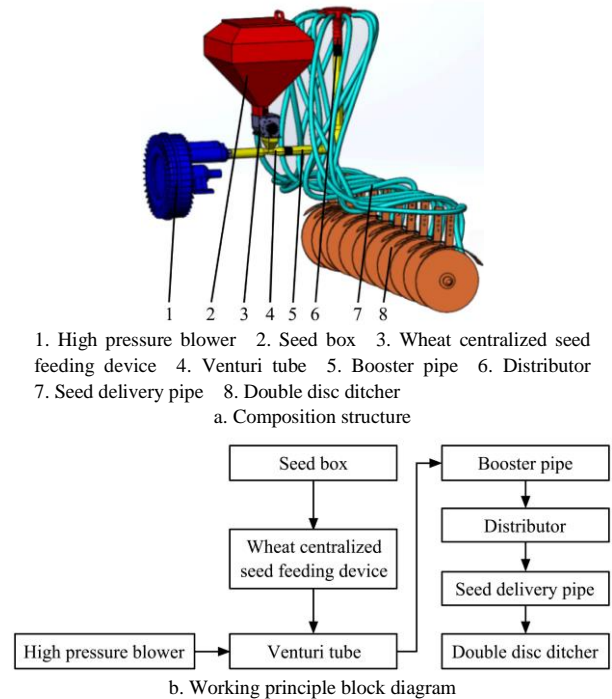
Figure 1   Working principle of air-assisted centralized seed feeding system

a. Structure of wheat centralized seed feeding device

b. Seed feeding mechanism
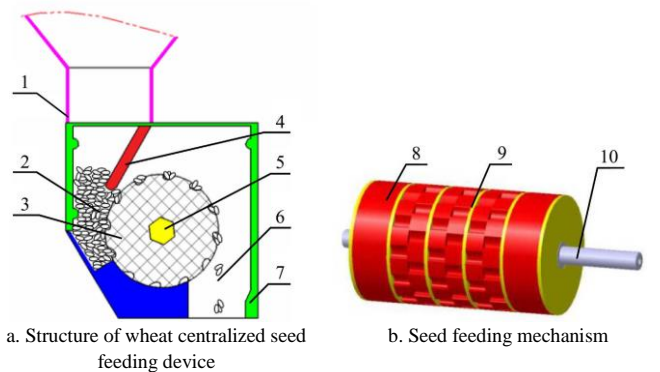
1. Seed box   2. Seed filling chamber   3. Type hole wheel   4. Seed filling adjusting board   5. Seed feeding mechanism   6. Seed fall mouth   7. Shell   8. Blank wheel   9. Clapboard   10. Transmission shaft

Figure 2   Sketch of wheat centralized seed feeding device

3 Materials and methods

3.1 Establishment of simulation model of wheat centralized seed feeding device

In order to explore the performance of the wheat centralized seed feeding device, the dynamic simulation model of the wheat centralized seed feeding device is built based on the DEM. Because the model structure is complex, some structures that do not affect the performance analysis are simplified. Select 100 seeds of three large-area wheat varieties planted in Huaibei plain, and measure their length, width and thickness, as shown in Table 1. Determine the geometric size of the grain model based on the average value of the triaxial size of the wheat, and establish the wheat model with seven spheres, as shown in Figure 3. According to the materials selected for a wheat centralized seed

feeding device, the shell is set as aluminum alloy, the type hole wheel is set as engineering plastic ABS (acrylonitrile butadiene styrene copolymer), the contact of the model is set as Hertz-Mindlin, and the relevant mechanical properties are obtained through the test, as shown in Table 2[7].

Table 1   Triaxial size of wheat seeds

Varieties	Length/mm	Width/mm	Thickness/mm
Yannong19	6.36	3.37	3.02
Bainong207	6.46	3.62	3.22
Wanmai68	6.46	3.24	2.90
Jimai22	6.35	3.37	3.10
Average	6.41	3.4	3.06

a. Wheat seed model

b. Simulation model of wheat centralized seed feeding device
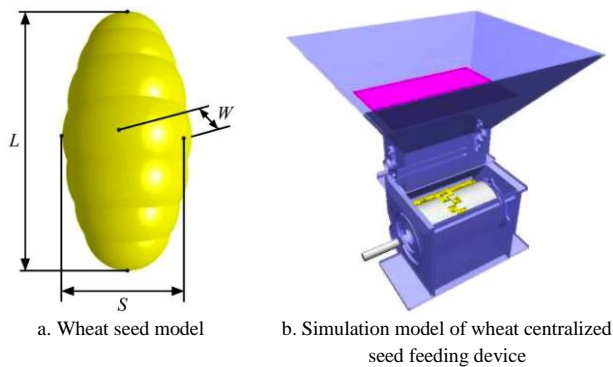
Figure 3   Simulation model

Table 2   Parameter setting of contact model between materials

Parameters properties	Parameters	Values
Particle properties	Density/kg·m^{-3}	822
	Poisson's ratio	0.42
	Shear modulus	5.1×10^7
Engineering material ABS properties	Density/kg·m^{-3}	1060
	Poisson's ratio	0.394
	Shear modulus	2.7×10^{10}
	Density/kg·m^{-2}	2700
	Poisson's ratio	0.3
	Shear modulus	8.96×10^8
Properties of aluminum alloy materials	Static friction coefficient between particles and particles	0.35
	Dynamic friction coefficient between particle and particle	0.05
	Recovery coefficient of particles and aluminum alloy	0.5
	Static friction coefficient between particles and aluminum alloy	0.4
	Dynamic friction coefficient between particles and aluminum alloy	0.05
	Recovery coefficient of particles and engineering plastics ABS	0.6
	Static friction coefficient of particles and engineering plastics ABS	0.4
	Dynamic friction coefficient between particles and engineering plastics ABS	0.05
Other parameters	Gravitational acceleration/m·s^{-2}	9.81
	Fixed time step/%	25
	Grid size/mm	4

3.2   Evaluation index of seed filling performance

This paper selects three evaluation indexes: average seed number of type hole, variation coefficient of the average seed number of type hole and maximum tangential force between seed and seed feeding mechanism.   The average seed number of type hole reflects the seed filling capacity of the seed feeding device, variation coefficient of the average seed number of type hole shows the seed filling stability of the seed feeding device, maximum tangential force between seed and seed feeding mechanism directly affects the damage rate of seeds.   In order to ensure the reliability of the data, the data within 3.0-8.0 s after the simulation test were extracted for analysis.   The calculation method of each evaluation index is as follows.

3.2.1   Average seed number of type hole

Select the total number of seed and the total number of type holes from 3.0 to 8.0 s, and calculate the average seed number of type hole.

$$Y_1 = \frac{M}{T} \qquad (1)$$

where, M is total number of seed; T is total number of type holes; Y_1 is average seed number of type hole.

3.2.2   Variation coefficient of average seed number of type hole

The number of seed filling particles in a single hole from 3.0 s to 8.0 s was extracted, the standard deviation was calculated, and the variation coefficient of the average seed number of type hole was calculated.

$$Y_2 = \frac{\bar{S}}{Y_1} \times 100\% \qquad (2)$$

where, $\bar{S}$ is standard deviation; Y_2 is variation coefficient of the average seed number of type hole.

3.2.3   Maximum tangential force between seed and seed feeding mechanism

The maximum tangential force between the seed and the seed feeding mechanism Y_3 in 3.0-8.0 s was extracted.

3.3   Simulation model verification

According to the test selection, the cone angle of type hole is 40°, the seed filling gap is 4mm, and the working speed is 50 r/min.   In order to extract parameters easily, set the number of type hole wheel in DEM as 1, simulation time as 8.0 s, and generate 3000 wheat seeds in the first 1.0 s.   At the 1.0 s, the type hole wheel starts to rotate, and the number of seeds in the 3.0-8.0 s type hole of Analyst post-processing module is extracted.   The comparison between simulation and the bench test is shown in Figure 4.   The bench test equipment is shown in Figure 5, mainly including bench, wheat centralized seed feeding device, TB86BL120-430 stepping motor (Changzhou Yuankong Ltd), i-SPEED 3 high-speed camera system (Japan OLYMPUS company), etc.   The test material is Bainong 207, with the mass of 1000 grains is 51.19 g and moisture content of 8.07%.   Select the same time period to extract data, calculate average seed number of type hole and variation coefficient of the average seed number of type hole.

Simulation and bench test results show that the model is accurate under the conditions of cone angle of type hole of 40°, seed filling gap of 0.004 m, working speed of 50 r/min, average seed number of type hole is 3.85 and 3.69, variation coefficient of the average seed number of type hole of 0.4612 and 0.4887, and the average error is less than 6%, as shown in Table 3.

Table 3   Verification test comparison

Type of test	Average seed number of type hole	variation coefficient of average seed number of type hole
Simulation test	3.85	0.4612
Bench test	3.69	0.4887
Error rate	4.3%	5.6%

a. 0.00 s   b. 0.25 s   c. 0.55 s

d. 0.95 s   e. 1.5 s   f. 2.0 s
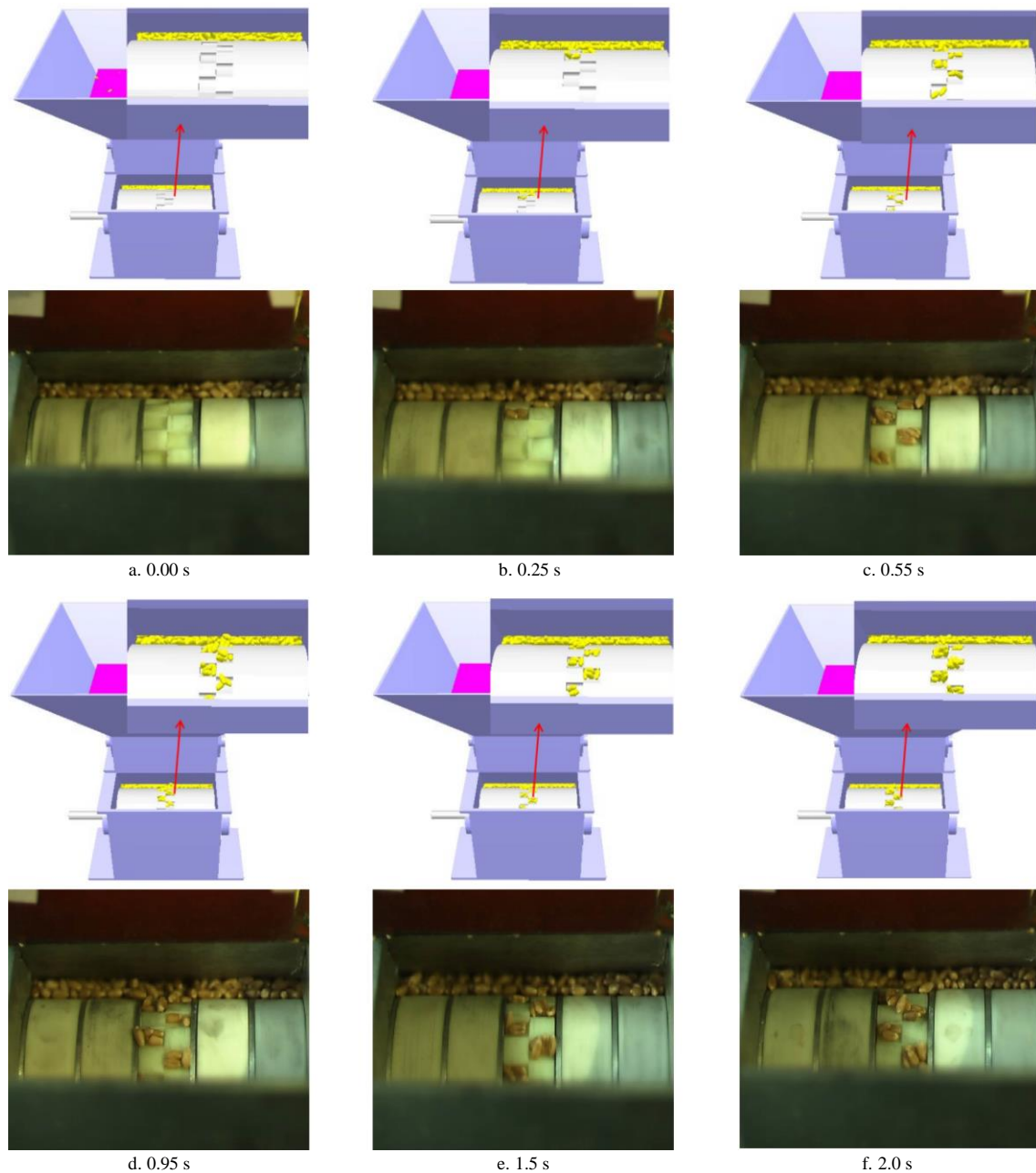
Figure 4   Comparison of simulation and bench test
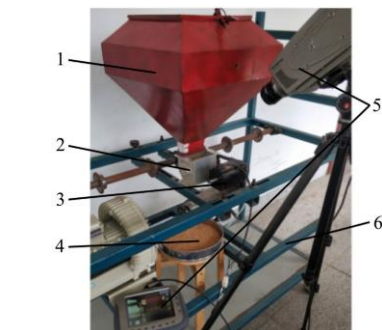
1. Seed box   2. Wheat centralized seed feeding device   3. Stepping motor
4. Aggregate device   5. High-speed camera system   6.Bench

Figure 5   Bench test

4   Effect of experimental factors on performance index of wheat centralized seed metering device

In order to further explore the influence of different parameters on the seed metering performance of wheat centralized seed feeding device, orthogonal experiments were performed with cone angle of type hole and seed filling gap as experimental structural parameters, working speed as operating parameters, and average seed number of type hole, the maximum tangential force between seed and seed feeding mechanism and variation coefficient of the average seed number of type hole as evaluating indicator.   The test factor level coding table is shown in Table 4.   Create simulation tests under different combinations through Table 4, and the results of the tests are shown in Table 5.

Table 4   Experimental factors and level codes

Level	Factors		
	X_1	X_2	X_3
1.682	50	70	0.006
+1	46	62	0.005
0	40	50	0.004
−1	34	38	0.003
−1.682	30	30	0.002

Note: X_1 is the code value of cone angle of type hole, (°); X_2 is the code value of working speed, r/min; X_3 is the code value of seed filling gap, m.

Table 5   Experimental project and results

Test No.	Factors			Index		
	X_1	X_2	X_3	Y_1	Y_2	Y_3
1	–1	1	–1	2.49	0.56	0.8164
2	0	0	–1.682	2.38	1.66	0.6542
3	1.682	0	0	3.32	0.0013	0.4107
4	0	0	0	3.85	0.044	0.4612
5	0	1.682	0	3.29	0.035	0.6602
6	–1.682	0	0	2.79	0.0064	0.5216
7	0	–1.682	0	3.65	0.007	0.3478
8	1	–1	1	4.06	0.035	0.3625
9	–1	–1	1	3.27	0.0012	0.4143
10	0	0	0	3.83	0.033	0.4826
11	–1	1	1	3.16	0.0046	0.7416
12	0	0	0	3.66	0.055	0.5532
13	1	–1	–1	3.77	0.43	0.5179
14	0	0	0	4.15	0.039	0.6602
15	–1	–1	–1	2.75	0.82	0.3602
16	0	0	1.682	3.42	0.02	0.4778
17	1	1	1	3.88	0.022	0.5581
18	1	1	–1	3.26	0.33	0.4861
19	0	0	0	3.79	0.027	0.534
20	0	0	0	3.97	0.029	0.5453

Note: Y_1 is the average seed number of type hole, grain; Y_2 is the maximum tangential force between seed and seed feeding mechanism, N; Y_3 is the variation coefficient of the average seed number of type hole.

Through the analysis of Y_1 data in Table 5, the variance analysis results of test factors on average seed number of type hole is shown in Table 6. From Table 6, the constructed model is 0.0008, lack of fit is 0.1371. The results show that the relationship between the average seed number of type hole and experimental factors is high significant, and the mismatch term is insignificant, which shows that the regression equation has a good fitting degree. The influence of cone angle of type hole and seed filling gap on the average seed number of type hole is high significant, the self intersection effect of the cone angle of type hole and the cone angle of type hole is high significant, the self intersection effect of seed filling gap and seed filling gap is high significant. The primary and secondary order of influence of each factor on the average seed number of type hole is $X_1 > X_3 > X_2$. The regression equation between each factor and index is obtained by removing the insignificant term, as shown in Equation (3).

$$Y_1 = 3.87 + 0.31X_1 + 0.28X_3 - 0.24X_1^2 - 0.3X_2^3 \qquad (3)$$

Through the analysis of Y_2 data in Table 5, the variance analysis results of test factors on maximum tangential force between seed and seed feeding mechanism are shown in Table 7. As can be seen from Table 7, the constructed model<0.0001. The results show that the dependent variable with maximum tangential force between seed and seed feeding mechanism as the test index has a significant quantitative relationship with all the independent variables with cone angle of type hole, working speed and seed filling gap as the test factors. The order of influence of each factor on maximum tangential force between seed and seed feeding mechanism is $X_3 > X_1 > X_2$. The regression equation between each factor and index is obtained by removing the insignificant term, as shown in Equation (4).

$$Y_2 = 0.039 - 0.35X_3 + 0.28X_3^2 \qquad (4)$$

Table 6   Analysis of variance of test factors to average seed number of type hole

Variation source	SS	df	MS	F	p
Model	4.57	9	0.51	9.35	0.0008**
X_1	1.29	1	1.29	23.71	0.0007**
X_2	0.20	1	0.20	3.74	0.0818
X_3	1.08	1	1.08	19.99	0.0012**
X_1X_2	0.013	1	0.013	0.24	0.6377
X_1X_3	9.8×10^{-3}	1	9.8×10^{-3}	0.18	0.6799
X_2X_3	0.029	1	0.029	0.53	0.4830
X_1^2	0.84	1	0.84	15.40	0.0028**
X_2^2	0.13	1	0.13	2.35	0.1563
X_3^2	1.26	1	1.26	23.20	0.0007**
Residual	0.54	10	0.054	–	–
Lack of fit	0.40	5	0.080	2.86	0.1371
Pure error	0.14	5	0.028	–	–
Total value	5.11	19	–	–	–

Note: SS is sum of squares; df is freedom; MS is mean squares; * shows this term is significant ($0.01<p<0.05$); ** shows this term is high significant ($p<0.01$). Same below. X_1, X_2, X_3 are the code value of the test factor.   Same as below.

Table 7   Analysis of variance of test factors to maximum tangential force between seed and seed feeding mechanism

Variation source	SS	df	MS	F	P
Model	2.98	9	0.33	16.14	<0.0001**
X_1	0.024	1	0.024	1.19	0.3008
X_2	7.616×10^{-3}	1	7.616×10^{-3}	0.37	0.5558
X_3	1.71	1	1.71	83.51	<0.0001**
X_1X_2	2.578×10^{-3}	1	2.578×10^{-3}	0.13	0.7303
X_1X_3	0.056	1	0.056	2.75	0.1284
X_2X_3	0.015	1	0.015	0.75	0.4072
X_1^2	4.643×10^{-3}	1	4.643×10^{-3}	0.23	0.6444
X_2^2	2.036×10^{-3}	1	2.036×10^{-3}	0.099	0.7591
X_3^2	1.11	1	1.11	54.20	<0.0001**
Residual	0.21	10	0.021	–	–
Lack of fit	0.20	5	0.041	369.84	<0.0001
Pure error	5.528×10^{-3}	5	1.106×10^{-4}	–	–
Total value	3.18	19	–	–	–

Through the analysis of Y_3 data in Table 5, the variance analysis results of test factors on variation coefficient of the average seed number of type hole are shown in Table 8. From Table 8, the constructed model is 0.0059, lack of fit is 0.4732. The results show that the relationship between the variation coefficient of average seed number of type hole and the experimental factors is high significant, and the mismatch term is insignificant, which indicate that the regression equation has a good degree to fit. The order of influence of each factor on variation coefficient of the average seed number of type hole is $X_2 > X_1 > X_3$. The regression equation between each factor and index is obtained by removing the insignificant term, as shown in Equation (5).

$$Y_3 = 0.54 - 0.044X_1 + 0.11X_2 - 0.077X_1X_2 \qquad (5)$$

5   Multi-objective optimization design of wheat centralized seed feeding device

5.1   Selection of design variables

Take cone angle of type hole, working speed and seed filling gap of wheat centralized seed feeding device as design variables.

$$X = [X_1, X_2, X_3] = [\sigma, n_p, H] \qquad (6)$$

where, X_1 corresponds to variable cone angle of type hole σ; X_2 corresponds to variable working speed n_p; X_3 corresponds to variable seed filling gap H.

Table 8   Analysis of variance of test factors to variation coefficient of the average seed number of type hole

Variation source	SS	df	MS	F	P
Model	0.26	9	0.029	5.72	0.0059**
X_1	0.026	1	0.026	5.18	0.0461*
X_2	0.16	1	0.16	31.79	0.0002**
X_3	0.012	1	0.012	2.35	0.1560
X_1X_2	0.048	1	0.048	9.61	0.0113**
X_1X_3	4.914×10^{-4}	1	4.914×10^{-4}	0.098	0.7602
X_2X_3	1.213×10^{-3}	1	1.213×10^{-3}	0.24	0.6329
X_1^2	6.547×10^{-3}	1	6.547×10^{-3}	1.31	0.2790
X_2^2	9.068×10^{-4}	1	9.068×10^{-4}	0.18	0.6791
X_3^2	2.820×10^{-3}	1	2.82×10^{-3}	0.56	0.4698
Residual	0.50	10	4.996×10^{-3}	–	–
Lack of fit	0.026	5	5.154×10^{-3}	1.07	0.4732
Pure error	0.024	5	4.838×10^{-3}	–	–
Total value	0.31	19	–	–	–

5.2   Constraint condition

5.2.1   Design of the cone angle of type hole

In order to obtain the parabola curve, it is necessary to combine the seed filling angle, seed dropping angle and the key dimension of the type hole structure of seed feeding device[20], and finally combine the position of the special point of the parabola to get the curve equation of the parabola as Equation (7), and the type hole structure is shown in Figure 6.

$$y = x^2 \quad (x \in [-1.5402, 2.8393]) \tag{7}$$
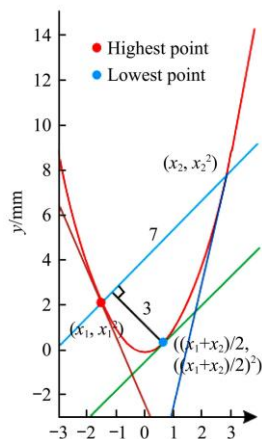
Figure 6   Structure curve of type hole

Due to the continuous movement of wheat seeds in the seed filling chamber in the form of discrete particles. The type hole can actively pick up multiple seeds with the rotation of the type hole wheel. Taking the particle system composed of multiple seeds filled into the type hole as the research object, it is assumed that the seeds are rigid bodies with uniform material, regardless of the friction and vibration between the research object and the population. The stress analysis is shown in Figure 7. The auxiliary coordinate system is established according to the normal and tangent directions of particle system motion, and its stress equation is as follows:

$$\begin{cases} N\cos\sigma = N_p \sin\alpha + f\sin\sigma + G\cos\alpha \\ F_t + G\sin\alpha \leq N_p \cos\alpha + f\cos\sigma + N\sin\sigma \\ f = \mu N \\ F_t = m\omega^2 R \\ G = mg \\ \omega = \pi n_p / 30 \end{cases} \tag{8}$$

where, N is support force of the side wall of the hole to the particle system, N; N_p is the lateral pressure of seed heap on the system of mass points, N; f is friction force between particle system and type hole wheel, N; F_t is inertial centrifugal force, N; G is gravity of particle system, N; m is mass of particle system, kg; α is initial seed filling angle, (°); σ is cone angle of type hole, (°); ω is angular velocity of type hole wheel, rad/s; R is radius of type hole wheel, m; μ is friction coefficient of contact surface between seed and wheel, take 0.55; n_p is working speed of type hole wheel, r/min; g is acceleration of gravity, m/s².
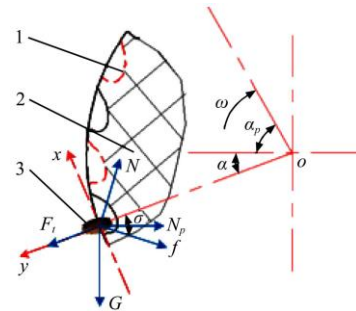
1. Type hole   2. Type hole wheel   3. Wheat seed

Figure 7   Mechanical analysis of wheat seed filling process

According to Equation (8), the redundant variables are eliminated and the relationship between the angular velocity of type hole wheel and the cone angle of type hole is obtained, as shown in Equation (9).

$$\alpha \geq \arccos \frac{\omega^2 R a}{g\sqrt{1+\mu^2}} - \arctan \frac{a}{b} \tag{9}$$

where, $a = \cos\sigma - \mu\sin\sigma$, $b = \mu\cos\sigma + \sin\sigma$.

Base on Equation (9), the initial filling angle is related to the cone angle of type hole, the seed material properties, the angular velocity and the diameter of the type hole wheel. When the angular velocity is determined, the initial seed filling angle α is inversely proportional to the hole cone angle of type hole σ. At the same initial seed filling angle α, positive correlation between the cone angle of type hole σ and the angular velocity ω of the type hole wheel; the initial filling angle α of wheat should be less than the natural angle of repose, that is $\alpha \leq 35°$. In order to avoid the phenomenon of "flying seed" in the process of seed filling. When the rotation speed of seed feeding mechanism is 10-100 r/min, the range of cone angle of type hole σ can be calculated as 8.02°-50.42°. Combined with previous tests, the range of selection cone angle of type hole is 30°-50°, that is:

$$30° \leq \sigma \leq 50° \tag{10}$$

5.2.2   Design of the seed filling gap

The particle system composed of several seeds in contact with the regulating plate is taken as the research object. Supposing that the seeds are rigid bodies with uniform material and the vibration between seeds is not considered. A mechanical model of seed filling process considering the effect of regulating plate is established, shown in Figure 8. According to the motion characteristics of the particle system, the auxiliary coordinate system is established, and the force formula is as Equation (11).

$$\begin{cases} F_N = F_{N2}\sin\sigma + f_1 + f_2 \\ F_{N1} + G_1 \geq F_T + F_{N2}\cos\sigma \\ f_1 = \mu_1 F_{N1} \\ f_2 = \mu F_{N2}\cos\sigma \\ G_1 = m_1 g \\ F_T = m\omega^2 (H/2 + R) \end{cases} \tag{11}$$

where, G_1 is weight of seed pile, N; θ is the angle between the gravity direction of particle system and the F_{N1} direction, (°); f_1 is friction between particle system and seed filling regulating plate, N; f_2 is friction between particle system and seed supply organization, N; F_N is the support of indoor seeds to the particle system, N; F_T is inertial centrifugal force, N; m_1 is mass of particle system, kg; H is seed filling gap, m; μ_1 is friction coefficient between wheat seed and aluminum alloy; F_{N1} is pressure of seed filling regulating plate on particle system, N; F_{N2} is the resultant force of the supporting force of the seed supply mechanism to the particle system, N; N_1 is support force of seed supply organization to particle system, N.
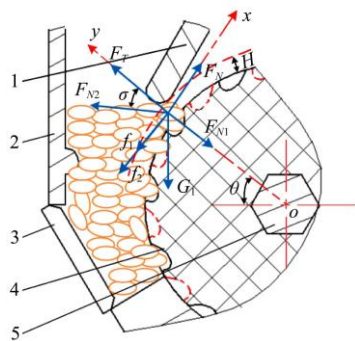
1. Seed filling adjusting board   2. Shell   3. Unloading seed plate
4. Type hole wheel   5. Transmission shaft

Figure 8   Mechanical analysis diagram of wheat in seed filling gap

Base on Equation(11), that is:

$$H \leq \frac{2(F_{N1} - G_1/\sin\theta - F_N\cos\sigma)}{m\omega^2} - 2R \qquad (12)$$

Base on Equation (12), the size of the seed filling gap H is related to the radius R of the hole wheel, the working speed of the type hole wheel, etc.   Taking into account the material characteristics of wheat and the common working speed of seed feeding mechanism 30-70 r/min, the seed filling gap can be calculated, $0.00186 \leq H \leq 0.00625$ m, that is:

$$0.002 \text{ m} \leq H \leq 0.006 \text{ m} \qquad (13)$$

5.2.3   Speed of seed feeding mechanism

Combined with a large number of experiments in the early stage and the general sowing amount of wheat, the working speed of the seed feeding mechanism is selected as 30-70 r/min, that is:

$$30 \text{ r/min} \leq n_p \leq 70 \text{ r/min} \qquad (14)$$

5.3   Establishment of objective function and multi-objective optimization

5.3.1   Establish objective function

One of the optimization objectives is the average number of type holes with higher feeding capacity of the feeding mechanism under the same working condition.

$$\min f_1(X) = 1/Y_1 = 1/(3.87 + 0.31X_1 + 0.28X_3 - 0.24X_1^2 - 0.3X_3^2) \quad (15)$$

Taking maximum tangential force between seed and seed feeding mechanism as one of the optimization objectives.

$$\min f_2(X) = Y_2 = 0.039 - 0.35X_3 + 0.28X_3^2 \qquad (16)$$

One of the optimization objectives is to reduce the variation coefficient of the average seed   number of type hole of type holes filled with seeds.

$$\min f_3(X) = Y_3 = 0.54 - 0.044X_1 + 0.11X_2 - 0.077X_1X_2 \qquad (17)$$

Based on the above objective functions, the total functions are established as follows:

$$\min f(X) = \omega_1 f_1(X) + \omega_2 f_2(X) + \omega_3 f_3(X) \qquad (18)$$

Among them, ω_1, ω_2, and ω_3 are weight coefficients, and their values are determined according to the conditions of each objective function, which are respectively taken as 0.3, 0.3, and 0.4.

5.3.2   Multi-objective optimization

Based on the PSO algorithm, Equation (18) is optimized.   The initial feasible solution number is 25, the population size is 100, the inertia weight is initialized to 0.95, the iterative algebra is 250, and the limit tolerance requirement is 10^{-5}.   The optimization results obtained after solving are shown in Table 9, and the optimization iteration is shown in Figure 9.

Table 9   Comparison before and after optimization

Parameters	Before optimization	After optimization	Rate of change
Cone angle of type hole	40	31.6	–21%
Working speed	50	50	0
Seed filling gap	0.004	0.0046	15%
Average seed number of type hole	3.85	3.72	–3.4%
Maximum tangential force between seed and seed feeding mechanism	0.044	0.037	–15.9%
Variation coefficient of the average seed number of type hole	0.4612	0.27	–41.5%
Objective function value	0.2312	0.1721	–25.56%
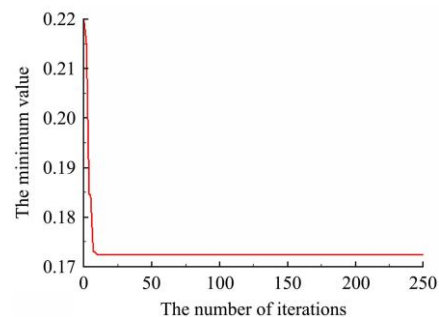
Figure 9   Iteration curve

6   Field test

The optimized type hole wheel were made by 3D printing technology.   Firstly, the bench test was carried out, the average number of hole particles and the variation coefficient of average seed number of type hole as the evaluation indexes.   The comparison of the margin between the evaluation indexes before and after optimization is shown in Figure 10.   It can be seen from Figure 10 that the margin between before and after optimization increases with the increase of working speed.

The field test was carried out in Huigu Town, Suzhou City, Anhui Province (116:97'E, 33:63'N) at Wanbei comprehensive test station of Anhui Agricultural University on October 19, 2018. The experimental area is corn field after cultivation.   During the test, the wheat centralized seed feeding device is controlled by the self-designed electric control feedback control system, and the motor drives the power 1:1 to the driving sprocket of the seed feeding device through the chain drive, so as to realize the quantitative seeding.   The width of the seeder is 2.2 m, the number of rows is 11, the traction power is FOTON LOVOL 900 tractor, and the driving speed is 5.4 km/h, Figure 11.   According to the requirements of farmers, three kinds of field experiments were carried out, which were 382.5 kg/hm², 322.5 kg/hm² and 170 kg/hm².   Seedling measurement was carried out on December 5, 2018, to measure the emergence rate of wheat under different sowing amounts, randomly select one square for plant measurement under different sowing amounts, randomly select three groups for measurement under the same sowing amounts, and the test data is shown in Table 10.   The coefficient of variation of uniformity was less than 16%, compared with 21.97% before optimization, it was improved by 37.3%.
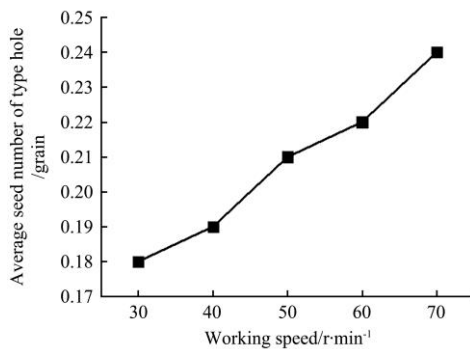
a. Average seed number of type hole
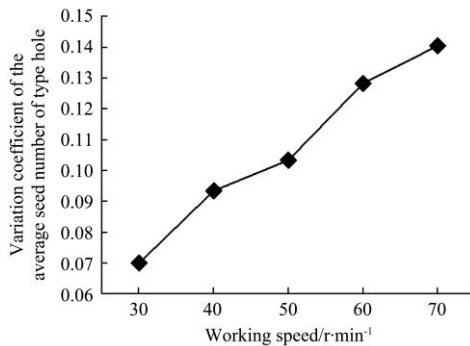
b. Variation coefficient of the average seed number of type hole

Figure 10   Margin before and after optimization

Figure 11   Field experiment and seedling situation

Table 10   Seedling measurement

Seeding rate /kg hm^{-2}	Average plant density/plant m^{-2}	Coefficient of variation for uniformity of each row/%
382.5	442	15.3
322.5	318	11.1
170	246	6.81

7   Conclusions and future work

(1) Through the simulation test, it is found that the effect of cone angle of type hole on maximum tangential force between seed and seed feeding mechanism is insignificant, and the effect of seed filling gap on maximum tangential force between seed and seed feeding mechanism is more significant, which provides guidance for using maximum tangential force between seed and seed feeding mechanism to study seed breakage rate.

(2) Compared with wheat centralized seed feeding device before and after optimization, the results of bench test show that the variation coefficient of the average seed number of type hole of wheat centralized seed feeding device after optimization are significantly reduced, and the field test shows that the uniformity variation coefficient of wheat centralized seed feeding device after optimization is higher than that before optimization 37.3%.

In addition to the factors considered in this paper, there are other external disturbances when the seed feeding device is operated in the field.   For example, the vibration of machines and tools caused by the uneven ground, the air pressure instability caused by the uneven tractor power and other factors will affect its seed metering performance.   Therefore, further research will be carried out on the performance of the centralized seed feeding device in the field operation.

Acknowledgements

[References]

[1]   Astahov V S.   Mechanical and technological fundamentals of the air-seeding having a centralized distribution system.   Doctoral dissertation, Gorki, Byelorussia, 2007; 377p.

[2]   Jat R A, Sahrawat K L, Kassam A H.   Conservation agriculture: Global prospects and challenges, 2013; Cabi, 424p.

[3]   Tow P, Cooper I, Partridge I, Birch C. (Eds.).   Rainfed farming systems. Springer Science & Business Media, 2011; 1336p.

[4]   Andrii Y, Jean-Pierre L, Frederic C.   Influence of the divider head functioning conditions and geometry on the seed's distribution accuracy of the air-seeder.   Biosystems Engineering, 2017; 161: 120–134.

[5]   Anantachara M, Prasanna Kumarb G V, Guruswamy T.   Development of artificial neural network models for the performance prediction of an inclined plate seed metering device.   Applied Soft Computing, 2011; 11: 3753–3763.

[6]   Karayel D, Wiesehoff M, Ozmerzi A, Muller J.   Laboratory measurement of seed drill seed spacing and velocity of fall of seeds using high-speed camera system.   Computers and Electronics in Agriculture, 2006; 50: 89–96.

[7]   Lei X L, Liao Y T, Liao Q X.   Simulation of seed motion in seed feeding device with DEM-CFD coupling approach for rapeseed and wheat. Computers and Electronics in Agriculture, 2016; 131: 29–39.

[8]   Lei X L, Liao Y T, Zhang Q S, Wang L, Liao Q X.   Numerical simulation of seed motion characteristics of distribution head for rapeseed and wheat. Computers and Electronics in Agriculture, 2018; 150: 98–109.

[9]   Liao Y T, Wang L, Liao Q X.   Design and test of an inside-filling pneumatic precision centralized seed-metering device for rapeseed.   Int J Agric & Biol Eng, 2017; 10(2): 56–62.

[10]   Zhang G Z, Zang Y, Luo X W, Wang Z M, Zhang Q, Zhang S S.   Design and indoor simulated experiment of pneumatic rice seed metering device. Int J Agric & Biol Eng, 2015; 8(4): 10–18.

[11]   Han D D, Zhang D X, Jing H R, Yang L, Cui T, Ding Y Q, et al. DEM-CFD coupling simulation and optimization of an inside-fifilling airblowing maize precision seed-metering device.   Computers and Electronics in Agriculture, 2018; 150: 426–438.

[12]   Liu J X, Wang Q J, Li H W, He J, Lu C Y.   Design and seed suction performance of pinhole-tube wheat precision seeding device. Transactions of the CSAE, 2019; 35(11): 10–18.

[13]   Zhou X Y, Shi Y J, Zhu J, Zhao L B, Zhu Z S.   Structural multi-objective optimization on a MUAV-based pan–tilt for aerial remote sensing applications.   ISA Transactions, 2020; 100: 405–421.

[14]   Hrvoje D, Tomislav P, Neven D.   Analysis of displacing natural gas boiler units in district heating systems by using multi-objective optimization and

different taxing approaches. Energy Conversion and Management, 2010; 205: 112411. doi: 10.1016/j.enconman.2019.112411.

[15] Paul R W, Nathan R M, Matthew J M. The use of multi-objective optimization to improve the design process of nuclear power plant systems. Annals of Nuclear Energy, 2020; 137: 107079. doi: 10.1016/j.anucene.2019.107079.

[16] Kihan K, Minsik S, Seungjae M. Efficient multi-objective optimization of gear ratios and motor torque distribution for electric vehicles with two-motor and two-speed powertrain system. Applied Energy, 2019; 259: 114190. doi: 10.1016/j.apenergy.2019.114190.

[17] Cai X W, Gao L, Li F. Sequential approximation optimization assisted particle swarm optimization for expensive problems. Applied Soft Computing Journal, 2019; 83: 105659.

[18] Ding Y M, Zhang Y, Zhang J Q, Zhou R, Ren Z Y, Guo H L. Kinetic parameters estimation of pinus sylvestris pyrolysis by Kissinger-Kai method coupled with Particle Swarm Optimization and global sensitivity analysis. Bioresource Technology, 2019; 293: 122079. doi: 10.1016/j.biortech. 2019.122079.

[19] Harrison K R, Ombuki-Berman B M, Engelbrecht A P. A parameter-free particle swarm optimization algorithm using performance classifiers. Information Sciences, 2019; 503: 381–400.

[20] Li Z D, Wang Q Q, Zhang Y L, Wang W W, Yang Y, Chen L Q. Design and test of inclined parabola-type hole wheel wheat seed feeder. Transactions of the CSAM, 2018; 49: 116–124.